[CANCER RESEARCH 62, 5698–5702, October 15, 2002]

Assessment of Proliferation *in Vivo* Using 2-[^{11}C]Thymidine Positron Emission Tomography in Advanced Intra-abdominal Malignancies[1]

Paula Wells, Roger N. Gunn, Malcolm Alison, Colin Steel, Mathew Golding, Alex S. Ranicar, Frank Brady, Safiye Osman, Terry Jones, and Pat Price[2]

Department of Cancer Medicine [P. W., P. P.], MRC Cyclotron Unit [R. N. G., C. S., A. S. R., F. B., S. O., T. J.], and Department of Histopathology [M. A., M. G.], Imperial College School of Medicine, Hammersmith Hospital, London W12 0HS, United Kingdom

ABSTRACT

The purpose of this study was to determine the relationship between 2-[^{11}C]thymidine positron emission tomography (PET) *in vivo*-derived parameters and the *ex vivo* Ki-67 index of proliferation in human tumors. The study comprised 17 treatment-naïve patients with advanced intra-abdominal malignancies. Tumor thymidine kinetics were measured using 2-[^{11}C]thymidine PET. Tissue data were analyzed to give the standardized uptake value, the area under the time activity curve, and the fractional retention of thymidine (FRT) obtained by kinetic modeling. For the latter, the contribution of labeled metabolites was accounted for by measuring thymidine metabolites in arterial plasma. To examine the influence of tumor blood flow on the thymidine PET data, a perfusion scan using inhaled [^{15}O]CO_2 was carried out in a subset of 11 patients. Biopsies were stained with a MIB1 antibody to obtain a Ki-67 index, and correlations with the PET-derived parameters were investigated. There was no relationship between tumor blood flow and the thymidine PET data, showing that the retention of 2-[^{11}C]thymidine in tumors was independent of tumor perfusion. There was no correlation between the Ki-67 index and either standard uptake value or area under the curve. There was a correlation between the Ki-67 index and FRT ($r = 0.58$; $P = 0.01$). The correlation between the Ki-67 index and FRT in this dataset was not influenced by the interval between biopsy and imaging (0.1–126 weeks), the origin of the biopsy for Ki-67 staining (primary tumor or metastasis), or whether the biopsy was from an imaged or a nonimaged tumor. This is the first report in human tumors showing that 2-[^{11}C]thymidine PET-derived parameters correlate with the level of tumor proliferation measured using Ki-67 immunohistochemistry. The study shows that the *in vivo* measurement of 2-[^{11}C]thymidine in tumors using PET can provide a surrogate marker of proliferation and supports the potential use of the technique in the early assessment of response to antiproliferative cancer treatment.

INTRODUCTION

In vivo metabolic imaging with PET[3] allows the diagnosis and assessment of therapeutic response in cancer patients (1). The most widely used PET radiotracer in oncology is the glucose analogue [^{18}F]FDG, which measures energy metabolism based on the rationale that FDG transport and phosphorylation are generally higher in tumor than in surrounding normal tissue. PET tracer development studies seek imaging agents with greater tumor selectivity and specificity for diverse tumor characteristics. The increased proliferation of tumor compared with surrounding normal tissue cells is a feature that has long been the target of antitumor drug and prognostic marker development. Whereas glucose is required by many cell types, particularly macrophages and other inflammatory cells that may be present in tumors (2), imaging proliferation rather than energy metabolism has the potential to be more selective for tumor cells. Moreover, DNA synthesis in tumors decreases after therapy more rapidly than FDG uptake (3), and hence a PET measure of tumor proliferation has the potential to provide a noninvasive tool for the early evaluation of antiproliferative treatment response (4). There are currently a number of PET radiotracers under development to provide a method for measuring human tumor proliferation *in vivo*.

There are a number of important issues relevant to determining the optimal PET tracer for imaging tumor proliferation. The interpretation of PET data can be complicated by the presence of labeled metabolites of the injected tracer. The position of the label on the tracer will influence the type and number of labeled metabolites, and the isotope half-life influences the quality of the PET data. The presence of a high concentration of labeled metabolites may mask the signal of the parent compound. Pyrimidine nucleoside incorporation into DNA has been used to study proliferation for many years. Thymidine and its analogues, such as the halogenated pyrimidines BrdUrd and IUdR, are particularly useful because of their specificity for DNA. Although the long half-life of [^{124}I]IUdR is attractive for protracted studies over several days, its use may be limited because of low tumor radioactivity compared with high levels of tissue metabolites (5). Similarly [^{76}Br]BrdUrd is extensively metabolized, and only a minor fraction of the radioactivity is found in DNA (6). The latter findings have driven a search for tracers that are metabolized less readily, such as [^{18}F]FLT (3′-deoxy-3′fluorothymidine; Ref. 7) and [^{11}C]FMAU (2′-fluoro-5-methyl-1-β-D-arabinofuranosyluracil; Ref. 8). It is labeled thymidine, however, that is currently the most widely studied proliferation marker for PET.

Initial attempts to use thymidine labeled in the methyl position yielded poor results because of a large number of labeled metabolites, and the method requires individual HPLC analysis of metabolites in blood samples (9). A better approach has been the use of thymidine labeled in the 2-C position that was developed initially by Vander Borght *et al.* (10, 11) and subsequently by Shields *et al.* (4, 12, 13). In comparison with methyl-labeled thymidine, 2-C-labeled thymidine yields fewer radioactive metabolites and yields metabolites that are less likely to be trapped in tissue and mistaken for labeled thymidine incorporated into DNA (10, 12). Although 2-C-labeled thymidine is metabolized *in vivo* at the same rate as the methyl derivative, [^{11}C]CO_2 is the main metabolite (11). Much of the labeled CO_2 is rapidly eliminated from the lungs (14), and what remains can be analyzed using developed methodology (15–17). In addition, kinetic modeling techniques have been developed that attempt to account for the confounding influence of the tissue metabolites (4, 18, 19). Preliminary studies have already described the potential of the method to measure proliferation (10) and tumor response to therapy (4).

Despite the publication of studies demonstrating the potential of 2-[^{11}C]thymidine PET, there are no reports correlating 2-[^{11}C]thymidine PET-derived parameters with conventional measures of proliferation in human tumors. The aim of the study reported here, therefore,

Received 4/28/02; accepted 8/15/02.

The costs of publication of this article were defrayed in part by the payment of page charges. This article must therefore be hereby marked *advertisement* in accordance with 18 U.S.C. Section 1734 solely to indicate this fact.

[1] Supported by grants from the Medical Research Council of the United Kingdom and Cancer Research UK.

[2] To whom requests for reprints should be addressed. Present address: Molecular Imaging Centre, Academic Department of Radiation Oncology, Christie NHS Trust Hospital, Wilmslow Road, Manchester M20 4BX, United Kingdom. Phone: 044-0-161-446-8003; Fax: 044-0-161-446-8111; E-mail: Anne.Mason@christie-tr.nwest.nhs.uk.

[3] The abbreviations used are: PET, positron emission tomography; FDG, fluorodeoxyglucose; IUdR, iododeoxyuridine; HPLC, high-pressure liquid chromatography; ROI, region of interest; SUV, standard uptake value; AUC, area under the curve; IRF, impulse response function; FRT, fractional retention of thymidine; BrdUrd, bromodeoxyuridine; CT, computed tomography.

was to further explore 2-[^{11}C]thymidine PET methodology as a marker of human tumor proliferation. The study was designed to measure tumor proliferation using 2-[^{11}C]thymidine in a series of patients with advanced intra-abdominal malignancies and correlate PET-derived parameters with a well-established immunohistochemical measure of tumor proliferation, the Ki-67 index (20).

MATERIALS AND METHODS

Patients. The study was approved by the ethical committee of the Imperial College School of Medicine, Hammersmith Hospital (London, United Kingdom). Permission to administer the radioactive tracers was obtained from the Administration of Radioactive Substances Advisory Committee of the United Kingdom. Patients with advanced intra-abdominal malignancies were enrolled, and all gave their written informed consent.

Production of Radiotracers. Production of [^{15}O]CO_2 was carried out by deutron bombardment of a ^{14}N target in a Scanditronic MC40 cyclotron. The gas was then exposed to a mixture of N_2 and CO_2 to produce [^{15}O]CO_2. All gaseous CO_2 produced was analyzed for radiochemical purity and sterility before administration. A detailed description of the method for producing 2-[^{11}C]thymidine has been given elsewhere (21). Formulations for i.v. injection were analyzed by HPLC to ensure chemical and radiochemical purity and by the Limulus amoebocyte lysate test to ensure apyrogenicity. Random samples were shown to be sterile.

Patient Imaging. Imaging was performed on an ECAT 931-08/12 scanner (CTI/Siemens, Knoxville, TN) after insertion of arterial and i.v. lines for blood sampling and injection of radiotracer, respectively. Patients were positioned on the scanner using skin markings of bony landmarks that were obtained using X-ray simulation of a ROI including the tumor that was defined from a CT scan. CT-PET image coregistration was not possible because of poor image alignment in the abdomen. To derive quantitative image data, results were calibrated and corrected for tissue attenuation and dead time. A ^{68}Ge phantom was used to calibrate the PET data with radioactivity measured in a well counter and enabled the image data to be expressed in kBq·ml^{-1}. An initial 20-min transmission scan was obtained for correction of tissue attenuation. In a subset of patients, the transmission scan was followed by a 10-min perfusion scan using inhaled [^{15}O]CO_2 (activity = 4 MBq) and a constant flow rate of 500 ml·min^{-1} for 210 s, starting 30 s into the scan. Arterial blood was withdrawn at a rate of 5 ml·min^{-1}, and radioactivity due to ^{15}O was monitored continually by passing the arterial whole blood through an on-line bismuth germinate detector cross-calibrated with a well counter (16, 22).

The 2-[^{11}C]thymidine scan was performed approximately 15 min after the perfusion scan. 2-[^{11}C]Thymidine was administered i.v. as a bolus over 30 s, 30 s after starting scanning. An on-line measuring system was used to record the radioactivity of arterial blood samples at 1-s intervals. Discrete blood samples were also taken up to 60 min after tracer administration to calibrate the radioactive counts, define the plasma to blood partitioning (n = 10), and measure the relative amounts of parent and metabolite compounds in the plasma (n = 6) using HPLC (23).

PET Image Analysis. The tomographic data were reconstructed using the method of filter back-projection. Voxel dimensions were 2.1 × 2.1 × 6.4 mm, and the radial, tangential, and axial full half width maximum values were 8.4, 8.3, and 6.6 mm, respectively. Inspection of a recent CT scan was used to assist the delineation of tumor and normal tissue regions. ROIs were defined using Analyze image analysis software (Biomedical Imaging Resource, Mayo Foundation) on integral images. To ensure only viable tumor was analyzed, tumor rims were defined using the conventional images, the perfusion scans, and the 2-[^{11}C]thymidine data. To minimize the effect of organ movement, tumor volume was defined on a minimum of five planes, avoiding those at the top and bottom and those at the apparent edge of an organ. All tumors greater than 4 cm^2 contained areas of central necrosis that were excluded from the ROIs (patients 4–7, 9–11, and 14–17). Once the ROIs were defined, they were applied to the dynamic images to generate time-activity curves for the tumor regions.

Quantification of Tissue Tracer Uptake. Changes in the imaged tumor tracer concentration measured over time, together with the plasma data, were used to estimate physiological parameters. In a subset of patients given [^{15}O]CO_2, values for tissue perfusion (ml·min·mg^{-1}) were obtained using the model described originally by Kety and Schmidt (24). A SUV was calculated for each time frame [SUV = measured tissue activity/(injected activity/patient weight)] from the start (t = 0) to the end (t = 3600 s) of the scan. The data were analyzed to give $SUV_{3000-3600}$ (kg·ml^{-1}) calculated as the midpoint between the SUV obtained at 3000 and 3600 s. The integral of the SUV time curve was used to calculate the area under the time-activity curve, AUC_{3600} (kg·min·ml^{-1}).

Kinetic modeling of the PET activity *versus* time data was carried out using spectral analysis, which fits a large number of discrete exponential curves to the data with no predefined compartments. Spectral analysis was used to calculate the tumor IRF using a plasma metabolite corrected input function and the corresponding tumor time-activity curve (15). Values for IRF were obtained for the delivery ($IRF_{1\ min}$) and the uptake ($IRF_{60\ min}$) of tracer in tumor. The FRT in tissue at 1 h was calculated as $IRF_{60\ min}/IRF_{1\ min}$. FRT values can range from 0–1, corresponding with 0–100% of the delivered tracer being retained in a tissue at 60 min.

Ki-67 Immunostaining. Before PET scanning, samples of the tumor to be imaged (the primary disease or a synchronously occurring metastasis) were taken for immunocytochemical analysis by MIB1 antibody staining. The antibody staining was performed on paraffin-embedded sections of tumor using published methodology (20). Briefly, after dewaxing and blocking endogenous peroxidase with 3% H_2O_2 for 20 min, sections were rinsed and immersed in boiling 10 mM citric acid (pH 6) and placed in a pressure cooker at 15 p.s.i. for 1 min. After rinsing further, sections were incubated with normal rabbit serum diluted 1:5 in PBS for 5 min, followed by 1 h with MIB1 antibody (Immunotech, S.A., Marseilles, France). Visualization of the antibody was obtained by incubation with conjugated streptavidin/biotin complex for 30 min followed by 0.5% diaminobenzidine and 0.03% H_2O_2 in PBS for 2–7 min. Finally, sections were counterstained with hematoxylin. Cell counting was performed without prior knowledge of the PET scan results. For each section, 2000 tumor cells were counted, and the number of nuclear-labeled tumor cells was expressed as a percentage of the total to provide the Ki-67 labeling index. The relationships between variables were investigated using the Pearson correlation coefficient.

RESULTS

Patient Characteristics. The study comprised 17 treatment-naïve patients with histologically confirmed advanced intra-abdominal malignancy. All patients had documented normal liver and renal functions. Tables 1 and 2 list the patient characteristics and PET variables. The mean age and weight were 65 years and 65 kg, respectively. The mean values with SDs for the injected radiotracer dose, radiochemical purity, and specific activity were 336 ± 145 MBq (range, 80–547 MBq), 99 ± 0.8% (range, 97.3–99.7%), and 19378 ± 13786 MBq/μmol (range, 5433–63060 MBq/μmol), respectively. The volume of tumor tissue imaged ranged from 2.8 to 17.6 cm^3 (mean, 7.5 cm^3).

Table 1 *Patient characteristics and Ki-67 index data*

Patient no.	Primary site	Imaged site	Gender	Age (yrs)	Weight (kg)	Biopsy from imaged tumor	Time (wks)[a]	LI (%)[b]
1	Anus	Primary	F	86	57	Y	2	42
2	Bowel	Ovary	F	69	51	Y	9	46
3	Liver[c]	Primary	M	49	89	Y	126	8
4	Bowel	Liver	M	67	75	Y	4	17
5	Bowel	Liver	M	61	50	N	22	64
6	Bowel	Liver	M	60	69	N	34	75
7	Unknown	Liver	M	62	90	N	0.1	42
8	Kidney	Lung	F	58	60	N	4	6
9	Bowel	Liver	F	59	60	Y	22	44
10	Bowel	Liver	F	56	58	N	9	52
11	Pancreas	Liver	F	65	67	N	86	32
12	Pancreas	Primary	F	59	62	Y	26	36
13	Pancreas	Primary	M	51	71	Y	4	34
14	Bowel	Liver	M	58	88	Y	2	63
15	Bowel	Liver	F	59	42	N	2	63
16	Bowel	Liver	M	76	84	Y	3	33
17	Bowel	Liver	F	69	37	Y	4	45

[a] Time, interval between biopsy for Ki-67 staining and scan.
[b] LI, Ki-67 index.
[c] Cholangiocarcinoma.

2-[^{11}C]Thymidine Distribution in Blood. Fig. 1 illustrates a typical time course for the distribution of 2-[^{11}C]thymidine in plasma. After a bolus injection of 2-[^{11}C]thymidine, the plasma radioactivity increased rapidly and reached a peak approximately 60 s after tracer administration. This was followed by a rapid fall in activity to approximately 5% of the starting value 5 min after injection. The percentage concentration of [^{11}C]CO_2, the predominant labeled metabolite, reached a plateau by 900 s and contributed 65–70% of all of the ^{11}C detected.

2-[^{11}C]Thymidine Distribution in Tissue. A rapid increase in tracer concentration was seen in all tissues and was followed by variable degrees of retention. Maximum tumor concentrations were seen 1–2 min after administration (Fig. 1). Tracer distribution was pronounced and most homogeneous in the tumor rims, aiding the definition of ROIs. ROIs drawn in normal tissues showed a rapid delivery of the tracer in the liver and spleen followed by slow washout, with faster clearance in the spleen. Rapid accumulation of 2-[^{11}C]thymidine was seen in the kidney followed by minimal clearance.

Analysis of the Influence of Tissue Perfusion on PET Data. Table 2 lists the tumor PET data obtained from the scans. Values for the FRT ranged from 0.096 to 0.690, with a mean of 0.343. In a subset of 11 patients, tumor blood flow ranged from 0.17 to 0.97 ml·min·mg^{-1}, with a mean of 0.52 ml·min·mg^{-1}. There was no significant relationship between tumor blood flow and the FRT ($r = -0.40$; Fig. 2).

Table 2 *PET data*

Patient no.	Tumor volume (cm^3)	SUV[a]	AUC[b]	FRT	IRF$_{60min}$[c]	Flow[d]
1	2.8	2.14	9.38	0.405	0.0015	0.65
2	4.1	1.64	7.26	0.635	0.0015	0.17
3	10.9	2.61	12.07	0.153	0.0011	0.46
4	6.6	0.98	8.73	0.240	0.0011	0.32
5	6.6	0.05	10.54	0.508	0.0027	
6	13.7	0.80	9.50	0.486	0.0059	0.35
7	9.6	0.04	13.16	0.295	0.0022	0.63
8	5.4	0.01	8.36	0.096	0.0003	0.66
9	4.4	0.02	7.99	0.274	0.0012	
10	17.6	0.04	13.41	0.197	0.0011	0.97
11	4.8	0.02	9.82	0.186	0.0009	0.18
12	5.7	0.06	12.44	0.189	0.0007	
13	9.4	0.09	9.84	0.578	0.0017	
14	2.9	0.02	5.81	0.690	0.0012	
15	6.8	0.01	9.66	0.276	0.0051	
16	11.2	0.05	14.83	0.372	0.0019	0.51
17	4.8	0.02	9.60	0.248	0.0018	0.52

[a] SUV, $SUV_{3000-3600}$ in kg · ml^{-1}.
[b] AUC in mg · min · ml^{-1}.
[c] IRF_{60min} in s^{-1}.
[d] Tumor blood flow in ml · min · mg^{-1}.

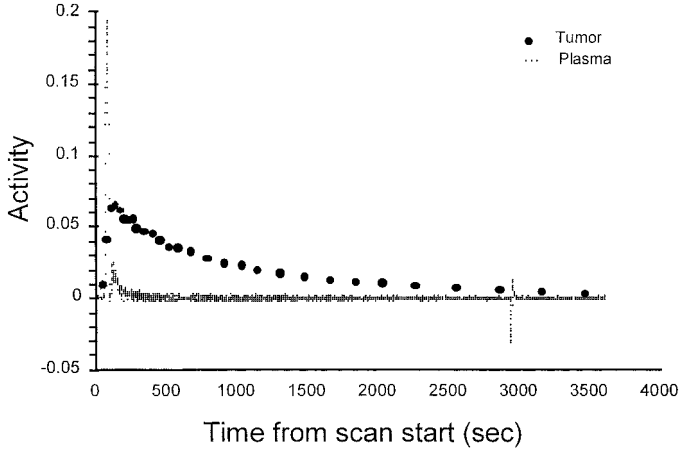

Fig. 1. The kinetics of 2-[^{11}C]thymidine uptake in blood and tumor in a patient with an advanced intra-abdominal cancer. Activity is the decay-corrected ECAT counts.

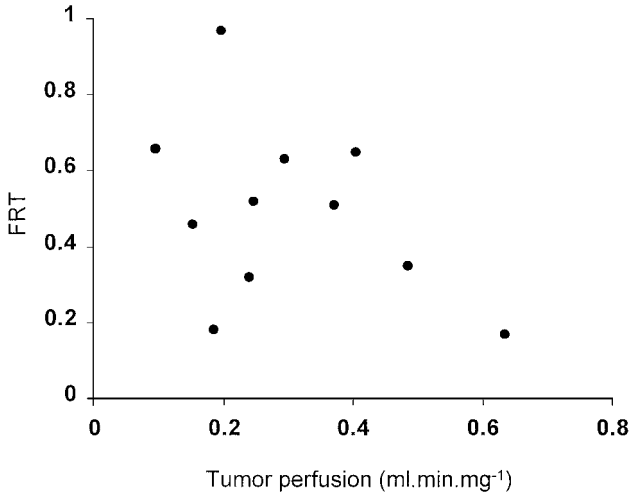

Fig. 2. The lack of relationship between the FRT and tumor perfusion. Data are for 11 patients given a [^{15}O]CO_2 perfusion scan followed by a 2-[^{11}C]thymidine proliferation scan.

Relationship with KI-67 Index. There was a wide range of values (6–75%) for the Ki-67 index (Table 1), with a mean of 42%. Fig. 3 illustrates the relationship between Ki-67 index and 2-[^{11}C]thymidine PET measurements of tracer incorporation. No significant relationship was seen between the Ki-67 index and either SUV or AUC. The $IRF_{60\ min}$ was also studied as a measure of the retention of the tracer. Although there was a correlation between $IRF_{60\ min}$ and Ki-67 index ($r = 0.68$; $P = 0.01$), it was skewed by two outlying points. There was a significant correlation between Ki-67 index and FRT ($r = 0.58$; $P = 0.02$) that was not influenced by outlying data points.

Influence of Biopsy Variables. The influence of biopsy variables was evaluated on the relationship between the tumor FRT and Ki-67 index (Fig. 4). The median interval between biopsy and PET scan was 4 weeks (range, 0.1–126 weeks; Table 1). Biopsies for Ki-67 staining were obtained from either nonimaged ($n = 7$) or imaged ($n = 10$) tumor. The correlation between the *in vivo* PET and *ex vivo* immunohistochemical measurement of tumor proliferation was not influenced by the timing of the biopsy (<4 weeks or >4 weeks before PET scan), the origin of the biopsy for Ki-67 staining (primary or metastasis), or whether the biopsy was from imaged or nonimaged tumor.

DISCUSSION

This study investigated the potential for 2-[^{11}C]thymidine PET to assess tumor proliferation *in vivo* in man. Heterogeneity was found in the tumor retention of 2-[^{11}C]thymidine between patients that was independent of blood flow. A study in mice showed that the initial distribution of thymidine measured 20 s after injection correlated with blood perfusion measurements, but all measurements of thymidine uptake made between 1 and 60 min after injection showed no correlation with perfusion (25). The work reported here has now shown in humans that the distribution of a thymidine tracer more than 1 min after injection is independent of tumor blood flow.

The analysis demonstrated no significant correlation between Ki-67 index and either SUV or AUC. The AUC is strongly influenced by data collected at an early time point because of the fall in activity within the ROI. This makes the AUC dependent on tracer delivery. Similarly, SUV does not correct for differences in the delivery of the tracer. The full potential of the PET technique requires the use of an appropriate model to relate the observed time course of the tracer in tissue to the concentration of tracer in plasma. The conventional approach to tracer kinetic modeling of PET data is to use a compart-

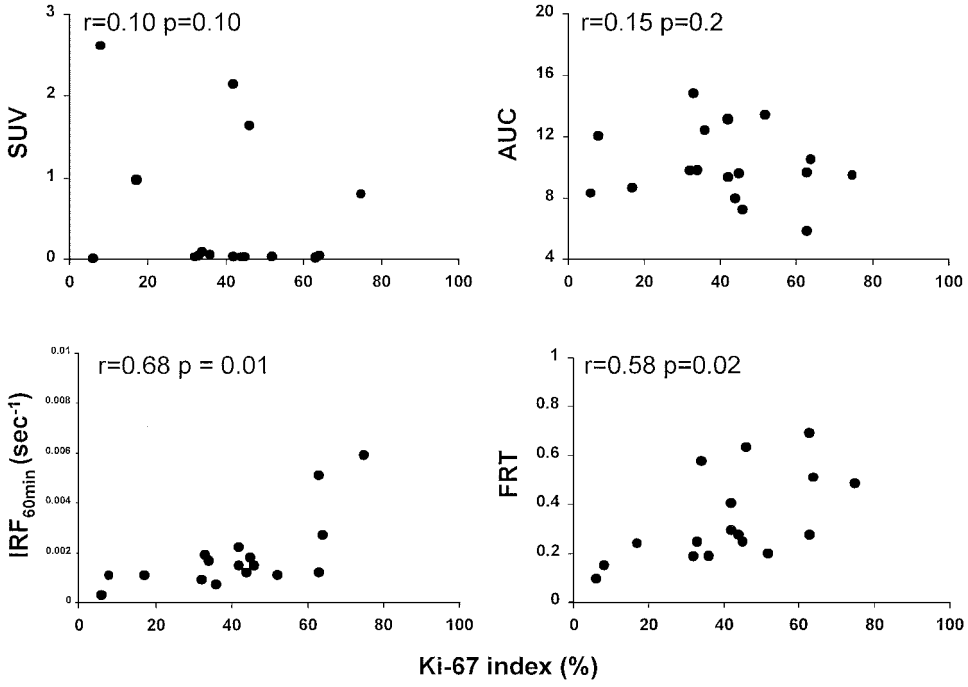

Fig. 3. The relationship of the *ex vivo* Ki-67 index of proliferation with the *in vivo* PET parameters SUV, AUC, $IRF_{60\ min}$, and FRT. Data are for 17 patients with advanced intra-abdominal malignancies.

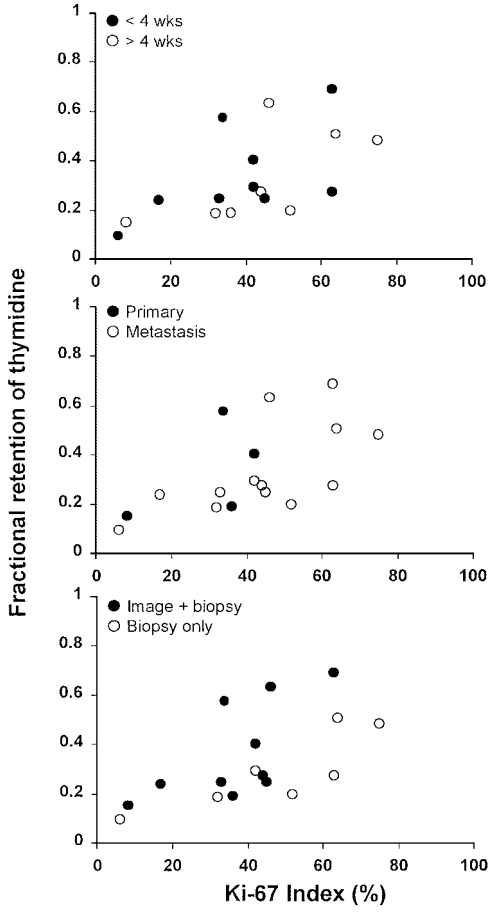

Fig. 4. Lack of influence of biopsy variables on the relationship between FRT and Ki-67 index. The relationship was not influenced by the interval between biopsy for Ki-67 staining and PET scanning (*top panel*), whether the biopsy was from the primary tumor or a metastasis (*middle panel*), or whether the biopsy was from the imaged or nonimaged tumor (*bottom panel*).

mental model with different compartments representing a particular tissue space or chemical form of the compound. Compartmental models require some knowledge of the biological fate of the compounds *in vivo*, and, because the number of compartments and relationships between them are fixed, they are highly constrained. If the assumptions are incorrect, then the model will be inaccurate. The model described by Mankoff *et al.* (18) included five tissue compartments requiring the estimation of eight rate constants from three measured blood input functions (thymidine, intermediate metabolites, and CO_2) and the time-activity curve. The latter approach can lead to a problem in identifying parameters. It was anticipated that it would not be possible to estimate all parameters accurately due to the similarity in time courses for each input function and the inherent noise in the tissue data. Spectral analysis (26) was therefore used to obtain pharmacokinetic parameters because it requires no *a priori* decision about the most appropriate compartmental structure (26–28). Spectral analysis allows for the characterization of the IRF of the tracer and accounts for the interpatient variability in tracer delivery.

The FRT parameter is related to the mean transit time of the tracer that equals the volume of distribution/delivery. The FRT is more robust to partial volume effects than other parameter estimates. Partial volume effects result from the limited spatial resolution of the tomograph. Thus, if a region contains tissue that is not homogeneous (for instance, where much of it is necrotic and lacks a signal), then the SUV and AUC parameters will underestimate the level of tracer incorporation. The FRT, however, will be independent of these partial volume effects. The FRT, like the other parameters, will still be susceptible to partial volume effects that relate to the spill in and out of regional signals due to the tomograph's inherent point spread function.

A relationship was seen between the level of tracer retained in tumors, measured using the spectral analysis, and Ki-67 index. Although the spectral analysis offers an improvement over SUV and AUC, it is important to note that none of the parameters obtained attempted to correct for the contribution of labeled metabolites in tissue. $[^{11}C]CO_2$ has been shown to comprise around 15% of the tumor activity (15), and the contribution of the other labeled metabolites is unknown. A method, based on a dual-scan approach, was

developed to correct for the presence of radiolabeled metabolites (15), but only after the data presented in this study were collected. It is likely, therefore, that there may be potential for improving the level of correlation between Ki-67 index and the *in vivo* measure of proliferation if further measurements of the metabolite contribution to the tissue could be made.

The $IRF_{60\ min}/IRF_{1\ min}$ ratio (FRT) appeared more robust than using $IRF_{60\ min}$. The correlation between Ki-67 index and FRT was similar to those reported for Ki-67 index and tritiated thymidine (29, 30), BrdUrd (31–33), and IUdR (34) indices. The wide range of Ki-67 indices seen in the cohort of patients studied was representative of a heterogeneous patient group, reflected by a similar range in values for FRT. The difference in tissue sampling techniques between the PET and pathology methods will contribute to the modest correlation between the parameters. For example, a tumor with a small number of highly proliferative cancer cells and a large number of nonproliferating normal cells (*e.g.*, fibroblasts, endothelial cells, macrophages, and lymphocytes) might appear less active using PET than a tumor with a high proportion of more slowly proliferating tumor cells and a small number of normal cells. A number of physiological and biological properties of tumors may also negatively influence the relationship between FRT and Ki-67 index. Some of the tissue samples were obtained many weeks before the PET study at the time of initial diagnosis. The biological variability between primary tumors and metastases may also be a confounding factor because of heterogeneity in the number of proliferating and metastasizing cells (35). In addition to the biological heterogeneity of these tumors that could potentially mask any true differences in proliferative behavior, physiological factors such as tumor perfusion may be important. The level of correlation seen between the Ki-67 index and FRT in the group of patients studied, despite the above-mentioned potentially confounding factors, supports the continued development of the methodology as a measure of human tumor proliferation.

In summary, this study has shown a statistically significant correlation between tumor FRT obtained *in vivo* using 2-[^{11}C]thymidine and proliferative index measured *ex vivo* using Ki-67 staining. The finding supports the use of 2-[^{11}C]thymidine PET as a means of measuring changes in tumor proliferation *in vivo* in response to antiproliferative treatment. This may be potentially useful in the selection or modification of treatment based on the individual biological characteristics of a tumor with the aim of improving treatment outcome.

REFERENCES

1. Wells, P., Harte, R. J., and Price, P. Positron emission tomography: a new investigational area for cancer research. Clin. Oncol., *8:* 7–14, 1996.
2. Kubota, R., Yamada, S., Kubota, K., Ishiwata, K., Tamahashi, N., and Ido, T. Intratumoral distribution of fluorine-18-fluorodeoxyglucose *in vivo*: high accumulation in macrophages and granulation tissues studied by microautoradiography. J. Nucl. Med., *33:* 1972–1980, 1992.
3. Kubota, K., Ishiwata, K., Kubota, R., Yamada, S., Tada, M., Sato, T., and Ido, T. Tracer feasibility for monitoring tumor radiotherapy: a quadruple tracer study with fluorine-18-fluorodeoxyglucose or fluorine-18- fluorodeoxyuridine, L-[methyl-^{14}C]methionine, [6-^{3}H]thymidine, and gallium-67. J. Nucl. Med., *32:* 2118–2123, 1991.
4. Shields, A. F., Mankoff, D. A., Link, J. M., Graham, M. M., Eary, J. F., Kozawa, S. M., Zheng, M., Lewellen, B., Lewellen, T. K., Grierson, J. R., and Krohn, K. A. Carbon-11-thymidine and FDG to measure therapy response. J. Nucl. Med., *39:* 1757–1762, 1998.
5. Blasberg, R. G., Roelcke, U., Weinreich, R., Beattie, B., von Ammon, K., Yonekawa, Y., Landolt, H., Guenther, I., Crompton, N. E., Vontobel, P., Missimer, J., Maguire, R. P., Koziorowski, J., Knust, E. J., Finn, R. D., and Leenders, K. L. Imaging brain tumor proliferative activity with [^{124}I]iododeoxyuridine. Cancer Res., *60:* 624–635, 2000.
6. Gudjonssona, O., Bergstrom, M., Kristjansson, S., Wu, F., Nyberg, G., Fasth, K. J., and Langstrom, B. Analysis of ^{76}Br-BrdU in DNA of brain tumors after a PET study does not support its use as a proliferation marker. Nucl. Med. Biol., *28:* 59–65, 2001.
7. Shields, A. F., Grierson, J. R., Dohmen, B. M., Machulla, H. J., Stayanoff, J. C., Lawhorn-Crews, J. M., Obradovich, J. E., Muzik, O., and Mangner, T. J. Imaging proliferation *in vivo* with [F-18]FLT and positron emission tomography. Nat. Med., *4:* 1334–1336, 1998.
8. Conti, P. S., Alauddin, M. M., Fissekis, J. R., Schmall, B., and Watanabe, K. A. Synthesis of 2′-fluoro-5-[^{11}C]-methyl-1-β-D-arabinofuranosyluracil ([^{11}C]-FMAU): a potential nucleoside analog for *in vivo* study of cellular proliferation with PET. Nucl. Med. Biol., *22:* 783–789, 1995.
9. Goethals, P., van Eijkeren, M., and Lemahieu, I. *In vivo* distribution and identification of ^{11}C-activity after injection of [methyl-^{11}C]thymidine in Wistar rats. J. Nucl. Med., *40:* 491–496, 1999.
10. Vander Borght, T., Lambotte, L., Pauwels, S., Labar, D., Beckers, C., and Dive, C. Noninvasive measurement of liver regeneration with positron emission tomography and [2-^{11}C]thymidine. Gastroenterology, *101:* 794–799, 1991.
11. Vander Borght, T., Labar, D., Pauwels, S., and Lambotte, L. Production of [2-^{11}C]thymidine for quantification of cellular proliferation with PET. Int. J. Radiat. Appl. Instrum. Part A, *42:* 103–104, 1991.
12. Shields, A. F., Lim, K., Grierson, J., Link, J., and Krohn, K. A. Utilization of labeled thymidine in DNA synthesis: studies for PET. J. Nucl. Med., *31:* 337–342, 1990.
13. Shields, A. F., Grierson, J. R., Kozawa, S. M., and Zheng, M. Development of labeled thymidine analogs for imaging tumor proliferation. Nucl. Med. Biol., *23:* 17–22, 1996.
14. Shields, A. F., Graham, M. M., Kozawa, S. M., Kozell, L. B., Link, J. M., Swenson, E. R., Spence, A. M., Bassingthwaighte, J. B., and Krohn, K. A. Contribution of labeled carbon dioxide to PET imaging of carbon-11-labeled compounds. J. Nucl. Med., *33:* 581–584, 1992.
15. Gunn, R. N., Yap, J. T., Wells, P., Osman, S., Price, P., Jones, T., and Cunningham, V. J. A general method to correct PET data for tissue metabolites using a dual-scan approach. J. Nucl. Med., *41:* 706–711, 2000.
16. Gunn, R. N., Ranicar, A., Yap, J. T., Wells, P., Osman, S., Jones, T., and Cunningham, V. J. On-line measurement of exhaled [^{11}C]CO_2 during PET. J. Nucl. Med., *41:* 605–611, 2000.
17. Shields, A. F., Mankoff, D., Graham, M. M., Zheng, M., Kozawa, S. M., Link, J. M., and Krohn, K. A. Analysis of 2-carbon-11-thymidine blood metabolites in PET imaging. J. Nucl. Med., *37:* 290–296, 1996.
18. Mankoff, D. A., Shields, A. F., Graham, M. M., Link, J. M., Eary, J. F., and Krohn, K. A. Kinetic analysis of 2-[carbon-11]thymidine PET imaging studies: compartmental model and mathematical analysis. J. Nucl. Med., *39:* 1043–1055, 1998.
19. Eary, J. F., Mankoff, D. A., Spence, A. M., Berger, M. S., Olshen, A., Link, J. M., O'Sullivan, F., and Krohn, K. A. 2-[C-11]Thymidine imaging of malignant brain tumors. Cancer Res., *59:* 615–621, 1999.
20. Key, G., Becker, M. H., Baron, B., Duchrow, M., Schluter, C., Flad, H. D., and Gerdes, J. New Ki-67-equivalent murine monoclonal antibodies (MIB 1–3) generated against bacterially expressed parts of the Ki-67 cDNA containing three 62 base pair repetitive elements encoding for the Ki-67 epitope. Lab. Investig., *68:* 629–636, 1993.
21. Steel, C. J., Brady, F., Luthra, S. K., Brown, G., Khan, I., Poole, K. G., Sergis, A., Jones, T., and Price, P. M. An automated radiosynthesis of 2-[^{11}C]thymidine using anhydrous [lsqb]^{11}C]urea derived from [^{11}C]phosgene. Appl. Radiat. Isot., *51:* 377–388, 1999.
22. Ranicar, A. S., Williams, C. W., Schnorr, L., Clark, J. C., Rhodes, C. G., Bloomfield, P. M., and Jones, T. The on-line monitoring of continuously withdrawn arterial blood during PET studies using a single BGO/photomultiplier assembly and non-stick tubing. Med. Prog. Technol., *17:* 259–264, 1991.
23. Luthra, S. K. Labelling of compounds with positron-emiting isotopes for PET studies. *In:* M. G. Stewart (ed.), Quantitative Methods in Neuroanatomy, pp. 117–161. New York: John Wiley and Sons, 1992.
24. Kety, S. S., and Schmidt, C. F. The nitrous oxide method for the quantitative determination of cerebral blood flow in man: theory, procedure and normal values. J. Clin. Investig., *27:* 476–486, 1948.
25. Shields, A. F., Larson, S. M., Grunbaum, Z., and Graham, M. M. Short-term thymidine uptake in normal and neoplastic tissues: studies for PET. J. Nucl. Med., *25:* 759–764, 1984.
26. Cunningham, V. J., and Jones, T. Spectral analysis of dynamic PET studies. J. Cereb. Blood Flow Metab., *13:* 15–23, 1993.
27. Meikle, S. R., Matthews, J. C., Brock, C. S., Wells, P., Harte, R. J., Cunningham, V. J., Jones, T., and Price, P. Pharmacokinetic assessment of novel anti-cancer drugs using spectral analysis and positron emission tomography: a feasibility study. Cancer Chemother. Pharmacol., *42:* 183–193, 1998.
28. Meikle, S. R., Matthews, J. C., Cunningham, V. J., Bailey, D. L., Livieratos, L., Jones, T., and Price, P. Parametric image reconstruction using spectral analysis of PET projection data. Phys. Med. Biol., *43:* 651–666, 1998.
29. Silvestrini, R., Costa, A., Veneroni, S., Del Bino, G., and Persici, P. Comparative analysis of different approaches to investigate cell kinetics. Cell Tissue Kinet., *21:* 123–131, 1988.
30. Veneroni, S., Costa, A., Motta, R., Giardini, R., Rilke, F., and Silvestrini, R. Comparative analysis of [^{3}H]-thymidine labelling index and monoclonal antibody Ki-67 in non-Hodgkin's lymphomas. Hematol. Oncol., *6:* 21–28, 1988.
31. Sasaki, K., Matsumura, K., Tsuji, T., Shinozaki, F., and Takahashi, M. Relationship between labeling indices of Ki-67 and BrdUrd in human malignant tumors. Cancer (Phila.), *62:* 989–993, 1988.
32. van Weerden, W. M., Moerings, E. P., van Kreuningen, A., de Jong, F. H., van Steenbrugge, G. J., and Schroder, F. H. Ki-67 expression and BrdUrd incorporation as markers of proliferative activity in human prostate tumour models. Cell Prolif., *26:* 67–75, 1993.
33. Lynch, D. A., Clarke, A. M., Jackson, P., Axon, A. T., Dixon, M. F., and Quirke, P. Comparison of labelling by bromodeoxyuridine, MIB-1, and proliferating cell nuclear antigen in gastric mucosal biopsy specimens. J. Clin. Pathol., *47:* 122–125, 1994.
34. Schipper, D. L., Wagenmans, M. J., Peters, W. H., Wobbes, T., and Wagener, D. J. Correlation between iododeoxyuridine and MIB-1 labelling index in gastric carcinoma and adjacent normal gastric tissue. Anticancer Res., *20:* 707–714, 2000.
35. Fidler, I. J. Critical factors in the biology of human cancer metastasis: twenty-eighth G. H. A. Clowes memorial award lecture. Cancer Res., *50:* 6130–6138, 1990.

Assessment of Proliferation *in Vivo* Using 2-[^{11}C]Thymidine Positron Emission Tomography in Advanced Intra-abdominal Malignancies

Paula Wells, Roger N. Gunn, Malcolm Alison, et al.

Cancer Res 2002;62:5698-5702.